JOURNAL OF Materials CHEMISTRY

Synthesis, structure and properties of a new ternary interstitial nitride: Ni_2W_3N†

P. Subramanya Herle,[a] M. S. Hegde,[a] K. Sooryanarayana,[a] T. N. Guru Row[a] and G. N. Subbanna[b]

[a]Solid State and Structural Chemistry Unit and [b]Materials Research Center, Indian Institute of Science, Bangalore-12, India

A new ternary interstitial nitride Ni_2W_3N has been synthesized by the ammonolysis of different oxide precursors and characterized by powder X-ray diffraction and electron microscopy. This nitride crystallizes in the cubic space group $P4_132$ (213) [Ni_2W_3N, $a=6.663(1)$ Å, $Z=4$] and is isostructural with Al_2Mo_3C. This compound belongs to the rare class of intermetallic ternary nitrides and carbides crystallizing with a filled β-Mn structure. Ni_2W_3N is not stable, it decomposes to a new compound NiW_3N related to the distorted anti-perovskite, Ca_3AsN structure.

Introduction

Metal rich nitrides, together with structurally closely related transition metal carbides, belong to the family of interstitial compounds. The common feature of these classes of materials is the simple metallic structures with the smaller nitrogen or carbon atoms in the interstitial voids. The unusual properties include exceptional hardness, high melting point with excellent electrical, thermal and magnetic properties.[1,2] Despite the potential technological importance of these materials, not many compounds are known, especially the ternary and higher ones, due to synthetic difficulties.[3] Interstitial nitrides containing two or more different metal atoms with widely different melting points are difficult to prepare by conventional methods involving high temperature treatment of metal powders in a nitrogen atmosphere because of the mass loss due to evaporation of the low melting point component. Therefore, low temperature routes are becoming important in synthesizing new nitrides in general. In recent years there has been increased interest in the synthesis of ternary transition metal nitrides from the oxide precursors.[4–6] Recently Weil and Kumta have reported Fe_3W_3N crystallizing with the η-carbide structure.[7] Our investigation on MWN_2 (M = Mn, Co, Ni)[6] from ammonolysis of the corresponding oxide precursors revealed the presence of a new intermetallic phase at higher synthetic temperatures. As part of a comprehensive research program into the ternary transition metal nitrides, we report here the first synthesis and structure of an interstitial metal nitride, Ni_2W_3N.

Experimental

The starting material $NiWO_4$ was prepared by dropwise addition of an aqueous solution of $NiCl_2$ (Alfa, 98.8%) to a solution of $Na_2WO_4\cdot 2H_2O$ (E. Merck, 98%). The hydrated $NiWO_4$ was filtered, washed in distilled water and ethanol and dried at 100 °C for 12 h. The ammonium heteropolynickelate(II) of tungsten was prepared by slow addition of nickel sulfate into a boiling solution containing appropriate amounts of $Na_2WO_4\cdot 2H_2O$.[8] The chemically complexed metallorganic hydroxide precursors were prepared using the stoichiometric inorganic metal chlorides $NiCl_2\cdot 6H_2O$, (Fluka, 99%) and WCl_6 (Fluka, 99%) in a dried acetonitrile medium with triethylamine as the complexing agent followed by hydrolysis of the viscous solution and removal of the solvent.[9] The title compound was synthesized by heating the precursor oxide in flowing ammonia gas (2.5 g in an alumina boat with a flow rate of *ca.* 150 ml min^{-1}) at different temperatures in a quartz tube. After the reaction the sample was quenched to room temperature and the product was examined by powder X-ray diffraction initially using a JEOL-8P powder X-ray diffractometer (Cu-Kα radiation). To check for nitride phase formation, the sample was heated under oxygen atmosphere in a temperature-programmed reaction (TPR) system attached to a VG QXK300 quadrupole mass spectrometer.[10] In a typical experiment, 200 mg of the oxide precursor was loaded and the reactor was evacuated to 10^{-6} Torr. Oxygen gas was admitted at about 15–20 μmol s^{-1} and the reactor was heated from 30 to 750 °C at a rate of 15 °C min^{-1}. The gaseous products were analyzed as a function of temperature. The quantitative nitrogen estimation was carried out employing a home-built thermogravimetric analyzer (TGA). The microstructures of the samples were studied using a Cambridge Scanning Electron Microscope (SEM) S-360, equipped with a LINK systems AN10000 X-ray analyser. The magnetic susceptibility of these samples was studied using a Lewis coil force magnetometer (field gradient 19 Oe cm^{-1}), and electrical properties were measured using a pressed pellet employing the four-probe technique.

Diffraction measurements

To study the crystal structure of this new phase in detail, intensity data for profile analysis were collected on a STOE/STADI-P powder X-ray diffractometer with Bragg–Brentano geometry (fine focus setting) using germanium monochromatised Cu-Kα_1 ($\lambda=1.54056$ Å) radiation in the 2θ range 5 to 76° at a step size of 0.02°. The pattern was indexed uniquely in a cubic cell with the PROSZKI program[11] and the cell dimension was refined to $a=6.658$ Å using the program REFINE (refinement of lattice constant) of the STOE/STADI-P diffraction system to a figure of merit of 45.4 (defined as $F(N)=1/[\text{av.}(2\theta)][N_{obs}/N_{pos}]$. N_{pos} is the number of independent diffraction lines possible up to Nth observed line). Rietveld refinements were carried out using a pattern fitting structure refinement (PFSR) package (a modified version of the original Rietveld program, which is compatible with the STOE X-ray diffraction system).[12] Electron diffraction patterns were obtained with a JEOL 200CX transmission electron microscope (TEM) to elucidate microstructural features.

† Contribution no. 1334 from the Solid State and Structural Chemistry Unit.

Results and Discussion

The previous investigation into ammonolysis of $NiWO_4$ at 600 °C gave $NiWN_2$ with metallic nickel as an impurity.[6] When $NiWO_4$ was heated in ammonia at 725 °C for 12 h, a new phase was observed with a small amount of metallic Ni [Fig. 1(a)]. This indicated the existence of a new phase hitherto unknown with an Ni/W ratio less than unity. To check for the nitrogen in the product we carried out a TPR experiment of the oxidation of the sample and Fig. 2(a) shows the TPR profile. We can see that N_2 was liberated at *ca.* 450 °C with simultaneous uptake of oxygen confirming the presence of nitrogen. From the literature studies on metal rich carbides and nitrides, compounds with molecular formula Ni_3W_3X (X = C, N) are not known.[13–16] However, Ni_3Mo_3C,[15] Fe_3Mo_3N,[5] Co_3Mo_3N[17] and Fe_3W_3N[7] crystallizing in the η-carbide structure are known. Since nickel phase segregation was observed during the ammonolysis of nickel tungstate, a nitride phase with a Ni : W ratio of 1 : 1 is not possible. EDX analysis of this sample did not give a conclusive result on the composition, as the particle size was small. This necessitated a careful analysis of the X-ray powder pattern to identify the new phase.

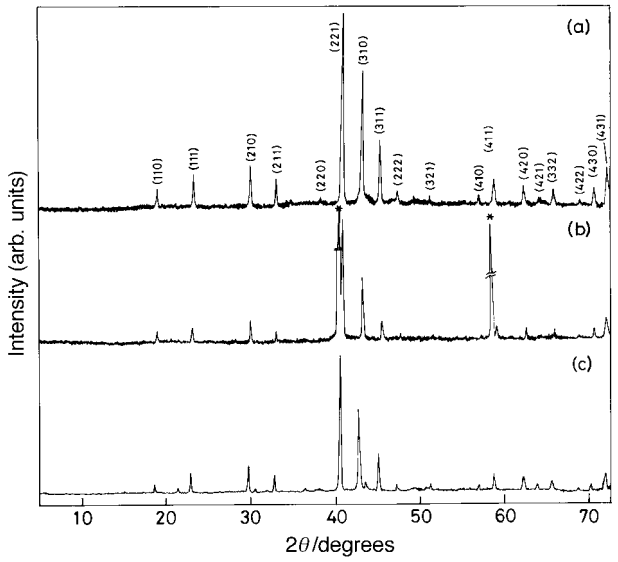

Fig. 1 Powder X-ray diffraction pattern of (a) $NiWO_4$ heated in ammonia at 725 °C for 12 h; (b) $(NH_4)_4[NiW_6O_{24}H_6]\cdot 5H_2O$ heated in ammonia at 800 °C for 12 h; (c) metallorganic precursor with a Ni : W ratio of 2 : 3 heated in ammonia at 950 °C for 12 h. The asterisks in (b) indicate tungsten metal.

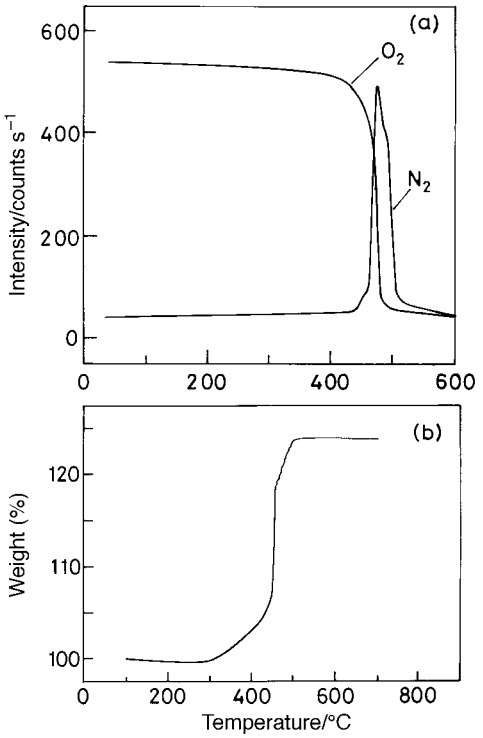

Fig. 2 Oxidation profiles for the nitride obtained from ammonolysis of $NiWO_4$ (725 °C, 12 h) (a) TPR profile; (b) TG profile

The X-ray powder diffraction of the nickel–tungsten–nitrogen phase was consistently indexed [Fig. 1(a)] in the $P4_132$ space group; by comparing the structure reports,[15,16] this phase was found to be isostructural with the Al_2Mo_3C phase.[18] The calculated intensity pattern for Ni_2W_3N, using Al_2Mo_3C as the structural model, agreed very well with the observed intensities. The TGA study of the sample was carried out in an oxygen atmosphere, assuming a biphasic mixture of $Ni_2W_3N_x$ and Ni. The oxidized product contained a mixture of NiO and WO_3. The mass gain of 23.93% against the expected 23.99% is consistent with the molecular formula $Ni_2W_3N_{1.03\pm0.02}$ and Fig. 2(b) shows the oxidation profile. The chemical equations for the ammonolysis of $NiWO_4$ and subsequent heating in an oxygen atmosphere can be given as:

$$6NiWO_4 + 16NH_3 \rightarrow 2Ni_2W_3N + 2Ni + 24H_2O + 7N_2 \quad (1)$$

$$2Ni_2W_3N + 2Ni + 12O_2 \rightarrow 6NiO + 6WO_3 + N_2 \quad (2)$$

When a mixture of Ni_2W_3N and Ni was heated further in ammonia a new set of X-ray peaks was observed. On heating $NiWO_4$ directly at 800 °C for 12 h in ammonia, a mixture of Ni_2W_3N and the new phase was observed. A systematic investigation led to the conclusion that, at higher temperatures, there exists another new phase with a lower Ni content; this new phase is referred to hereafter as phase (II). When the sample was heated in ammonia for a prolonged period, the Ni_2W_3N peak intensities were diminished and peaks for phase (II) appeared simultaneously [Fig. 3(a)–(d)]. To investigate phase (II), we have heated $(NH_4)_4[NiW_6O_{24}H_6]\cdot 5H_2O$ in

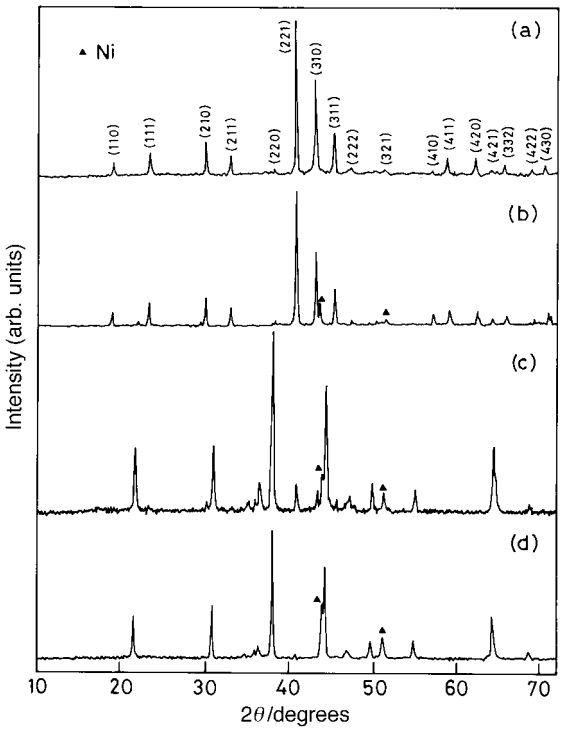

Fig. 3 Powder X-ray diffraction of $NiWO_4$ heated in ammonia at different temperatures with intermittent grindings. (a) 750 °C for 12 h; (b) 800 °C for 12 h; (c) 800 °C for 48 h with intermittent grindings; (d) 800 °C for 72 h with intermittent grindings.

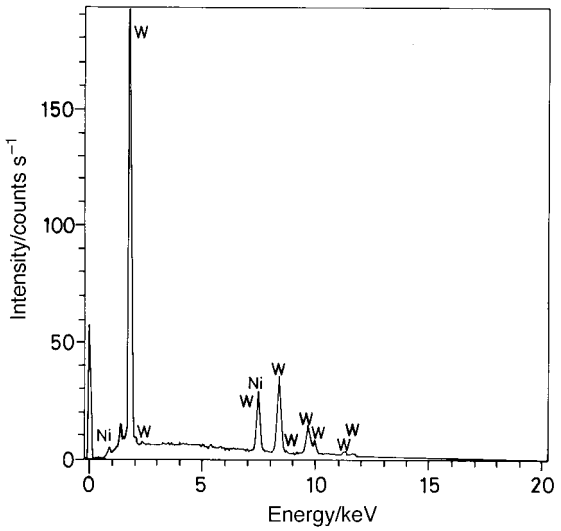

Fig. 4 EDX profile of the product obtained from ammonolysis of metallorganic precursor at 950 °C for 12 h; Ni (atom%) = 39.46; W (atom%) = 60.54

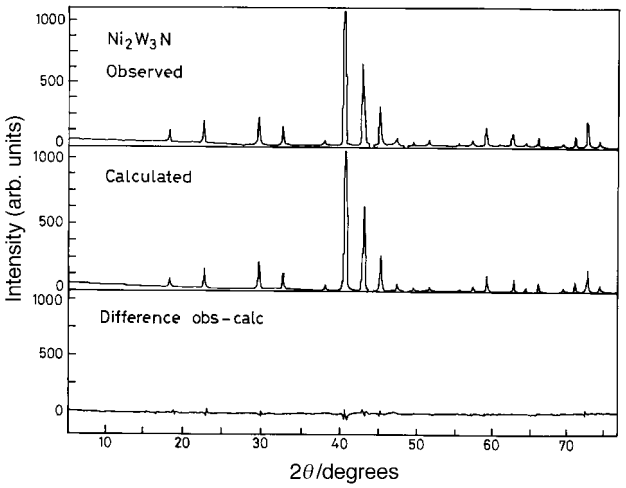

Fig. 5 Observed and calculated X-ray diffraction pattern (Cu-Kα_1 radiation) together with difference plot of Ni_2W_3N

Table 2 Crystallographic data and structural refinements for Ni_2W_3N

empirical formula	Ni_2W_3N
formula mass	682.956
crystal system	cubic
space group	$P4_132$
a/Å	6.663(1)
volume/Å^3	295.84
Z	4
$F(000)$	1140
D/g cm^{-3}	15.364
radiation; λ/Å	Cu-Kα_1; 1.54056
2θ range; step size/°	5–80; 0.02
excluded regions	
I	43.5, 44.22
II	48.2, 48.88
measurement time/s step^{-1}	5
refinement method	Rietveld on F^2
profile function	Pearson V11 with exponent 2.0
$R_{I,hkl}$ (%)	12.3
R_p (%)	11.0
R_{wp} (%)	15.4
diffraction method	transmission mode
diffractometer	STOE-STADI/P

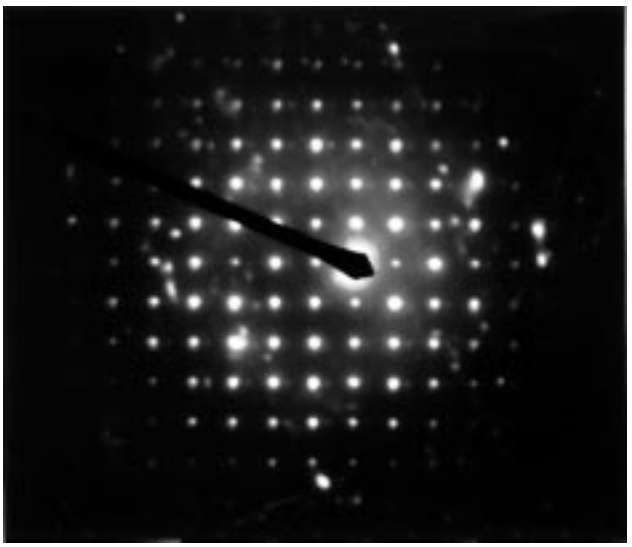

Fig. 6 Electron diffraction pattern along the [001] zone axis for Ni_2W_3N

ammonia at different temperatures. Fig. 1(b) shows the powder X-ray pattern of the final product, and it is clear that the heteropolynickelate(II) precursor gives a mixture of Ni_2W_3N and W at 800 °C. However, on further heating in ammonia Ni_2W_3N decomposed to phase (II). It is clear from the above observation that Ni_2W_3N is not stable, but undergoes slow decomposition. It is interesting to note that the excess tungsten in the precursor was not converted into the normally expected W_2N phase.

Attempts were made to obtain single-phase Ni_2W_3N from the chemically complexed metallorganic precursor with an Ni : W ratio of 2 : 3; the precursor was heated in ammonia at different temperatures. At 950 °C for 4 h, a mixture of Ni_2W_3N and a small amount of phase (II) was observed, probably due to the higher synthetic temperature [Fig. 1(c)]. However, EDX analysis confirmed the Ni : W ratio of 2 : 3 as the major phase and the EDX profile of this phase is shown in Fig. 4. At low synthetic temperatures there were some unidentified broad peaks along with those of Ni_2W_3N. Experimental details of all these studies are summarized in Table 1.

Rietveld refinement of the Ni_2W_3N sample, prepared from $NiWO_4$ heated in ammonia at 725 °C for 12 h, was carried out with $P4_132$ as the space group and the Ni impurity peaks were excluded (Table 2). The thermal parameter of nitrogen was fixed at 0.06 Å^2 while all the parameters of Ni and W were allowed to refine freely. The occupancy refinement of Ni and W showed full occupancy of those atoms at the 8c and 12d sites. The refinement converged with $R_{I,hkl} = 12.3\%$, $R_p = 11.0\%$, $R_{wp} = 15.4\%$ and $\chi^2 = 3.9$. Due to the small size of the particles [see Fig. 7(a) later], it is difficult to converge the

Table 1 Summary of ammonolysis of different oxides

precursor	ammonolysis condition	products
$NiWO_4$	725 °C, 12 h	$Ni_2W_3N + Ni$
$NiWO_4$	800 °C, 12 h	$Ni_2W_3N + NiW_3N + Ni$
$NiWO_4$	800 °C, 72 h	$NiW_3N + Ni$
$(NH_4)_4[NiW_6O_{24}H_6]\cdot 5H_2O$	800 °C, 12 h	$Ni_2W_3N + W$
(Ni_2W_3) metallorganic precursor	950 °C, 4 h	$Ni_2W_3N + NiW_3N + Ni$

Table 3 Atomic parameters for Ni_2W_3N

atom	position	x/a	y/b	z/c	$U_{iso}/Å^2$	occupancy
W	12d	0.2005(6)	0.4505(6)	1/4	0.027(8)	1.0
Ni	8c	0.068(2)	0.068(2)	0.068(2)	0.012(3)	1.0
N	4a	3/8	3/8	3/8	0.06	1.0

bond distances/Å; bond angles/°

$[NW_6]$ octahedra	$Ni[Ni_3W_9]$ polyhedra	$Mo[N_2Ni_6W_6]$ polyhedra
N—W × 6 2.092(2)	Ni—Ni × 3 2.4739(2)	W—N × 2 2.092(2)
	Ni—W × 3 2.721(4)	W—Ni × 2 2.721(4)
W—N—W × 6 83.30(2)	Ni—W × 3 2.770(2)	W—Ni × 2 2.770(3)
W—N—W × 3 85.70(2)	Ni—W × 3 2.828(4)	W—W × 4 2.781(3)
W—N—W × 3 111.4(1)		W—Ni × 2 2.828(3)
W—N—W × 3 160.40(1)		W—W × 1 2.846(5)
		W—W × 1 3.459(1)

refinement further to lower values of $R_{I,hkl}$, R_p and R_{wp}. Results of the refinements and the atomic positions are listed in Table 3 along with selected bond distances and bond angles. Fig. 5 shows a comparison of the experimental plot with that obtained by refinement, along with the difference plot.

Transmission electron microscopy studies confirmed the cubic structure of Ni_2W_3N. The electron diffraction pattern is shown in Fig. 6 along the [001] zone axis. The lattice parameter matches well (*ca.* 6.7 Å) with that found from the X-ray diffraction study.

Fig. 7(a) shows the SEM photograph of Ni_2W_3N obtained from ammonolysis of $NiWO_4$ at 725 °C for 12 h. It is clear that the particles are small and their size is in the sub-μm range. Fig. 7(b) shows phase (II) obtained from prolonged heating. It is clear that the crystallites are large and are in the μm size range. We could clearly detect Ni particles segregated on the surface of the larger particles. For comparison, the Ni–W metallorganic precursor heated in ammonia at 950 °C is shown in Fig. 7(c). The precursor shows a different morphology to that of Ni_2W_3N [*cf.* Fig. 7(a)], the porous nature of the particles being due to the enormous volume reduction of the precursor during ammonolysis.

TPR studies of phase (II) confirmed the presence of nitrogen in the system. The molecular formula from EDX analysis can be given as NiW_3N. Though the major intense lines in the powder diffraction pattern [Fig. 3(d)] could be indexed to a simple cubic cell with $a = 4.111(1)$ Å, using the program REFINE with a high figure of merit (120), the small peaks were not accounted for by any impurity phases comprised of Ni–W alloy phases or the corresponding binary nitrides. On careful analysis, all the peaks in Fig. 3(d), excluding metallic nickel peaks, could be indexed using a slightly different indexing scheme, and the new cell is orthorhombic with $a = 5.799(1)$ Å, $b = 5.827(1)$ Å and $c = 8.245(2)$ Å (Table 4). These orthorhombic cell parameters are closely related to the cubic cell parameter, since $a \approx b \approx 4.111 \times \sqrt{2}$ Å and $c \approx 2 \times 4.111$ Å. The corresponding structural model for such a system was found to be Ca_3AsN.[19] Ca_3AsN is a distorted anti-perovskite having an orthorhombic cell with $a \approx b \approx \sqrt{2} \times a'$ and $c \approx 2a'$, where a' is the lattice constant of the ideal undistorted cubic anti-perovskite. Intensity calculations using the Lazy Pulverix program for NiW_3N with Ca_3AsN as the structural model (Ni and W atoms are fixed to As and Ca positions respectively) agree reasonably well with the observed intensity.

The general formula for the filled β-Mn[20] structure can be given as A_2M_3X where A generally refers to a non-transition metal and M is a transition metal; X can be carbon or nitrogen. Similarly η-carbide structure can be given as $M_3M'_3X$ (X = C,N,O) where M is a transition metal atom and M′ can be a transition metal atom or a non-transition metal atom. The unit cell dimension of β-Mn is *ca.* 6.5–7 Å, whereas that of η-carbide is *ca.* 11–12 Å. Both structure types can be classified as Nowotny octahedral phases in which the metal substructure is no longer close packed with the non-metal in an octahedral site; the crystal structures of these ternary phases are best described in terms of geometric arrangements of these octahedra.[1] All interstitial compounds belonging to the η-carbide and β-Mn families have the common feature that the non-metal atom occupies an octahedral interstitial site surrounded by transition metal atoms. However, there is an important distinction between the two structure types. In the case of the η-carbide structure[1] the regular octahedra share corners with both metal atoms in the pseudo-icosahedral coordination whereas in the case of the β-Mn structure the slightly distorted octahedra share corners with the non-transition metal atoms in pseudo-icosahedra and transition metal atoms in pseudo-tetradeca-hedron coordination. Fig. 8 shows a structural model of the Ni_2W_3N unit cell and the arrangement of the octahedra. Fig. 9(a) shows the $[NW_6]$ distorted octahedra. Nickel atoms are located in 12-fold, pseudo-icosahedral coordination, surrounded by nine tungsten and three nickel atoms to give $Ni[W_9Ni_3]$ polyhedra: Fig. 9(b) shows $Ni[W_9Ni_3]$ pseudo-icosahedra in Ni_2W_3N. Molybdenum atoms are in pseudo-tetradecahedron sites with two nitrogens, and six nickel and molybdenum atoms to give $W[N_2Ni_6W_6]$ polyhedra [Fig. 9(c)].

The surprising feature about the η-carbide structure is the wide selection of transition elements originating from different parts of the Periodic Table.[13] In the case of nitrides, the η-carbide structure is common whereas compounds crystallizing with the β-Mn structure are rare. It may be recalled that Fe_3Mo_3N, Co_3Mo_3N and Fe_3W_3N crystallize with the η-carbide structure and also the molybdenum compounds are synthesized from the ammonolysis of the corresponding $MMoO_4$ (M = Fe, Co)[5,17] precursor. It is important to note that the nickel compound does not crystallize in the η-carbide structure. Nickel stands apart from the iron and cobalt containing interstitial compounds, possibly due to the different sizes of the atoms and electrochemical factors.[21]

The number of anti-perovskites with the molecular formula $M_3M'X$, where the positions of the anions and cations are reversed from perovskites, *i.e.*, X and M′ are generally anions and M is a cation, is much smaller than that of normal perovskites having the corner-shared NM_6 regular octahedral network extended to three dimensions.[15,16,19] In the perovskite structure the regular NM_6 octhedra are linked by sharing corners and form a simple cubic array, but the network with slightly distorted NM_6 octahedra lowers the symmetry.[22] The NiW_3N compound is not a regular anti-perovskite, possibly due to the presence of distorted NM_6 octahedra. X-Ray photoelectron spectroscopic (XPS) studies on these samples

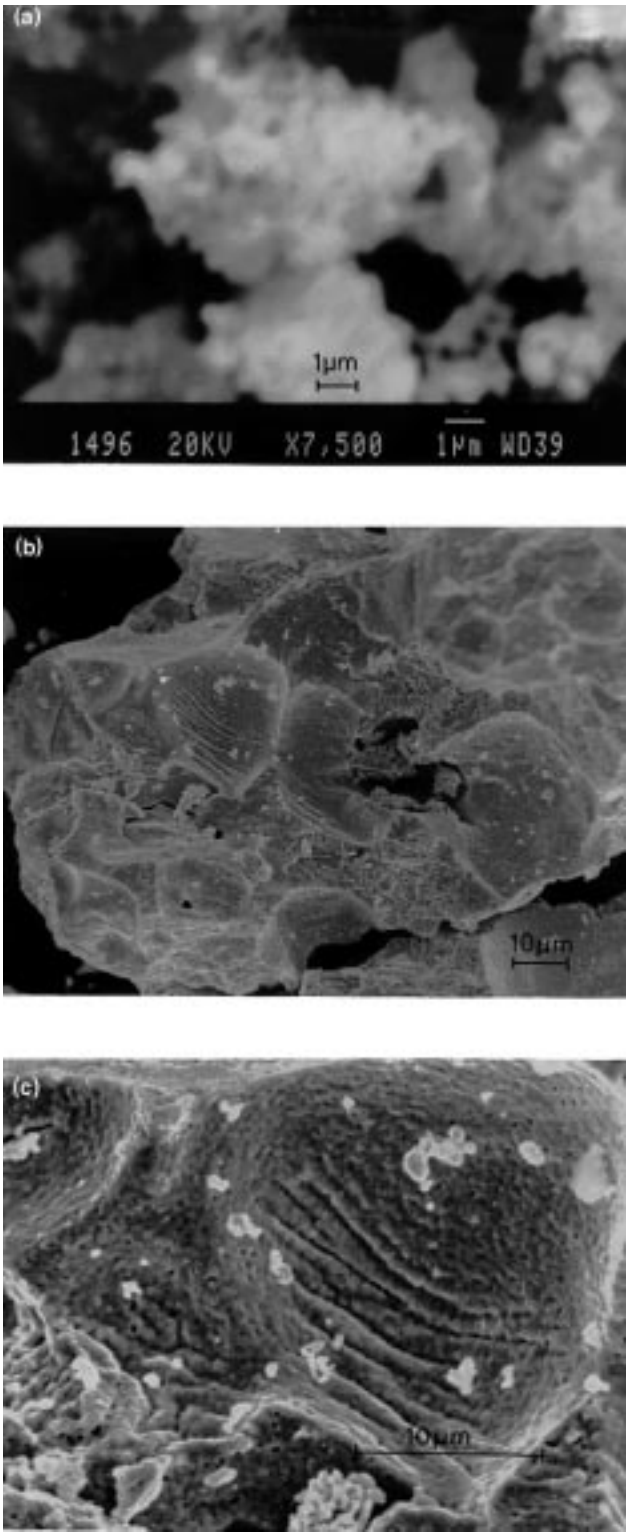

Fig. 7 SEM images showing microstructures of heat-treated ternary nitride powders. (a) Ni_2W_3N obtained from ammonolysis of $NiWO_4$ at 725 °C for 12 h and (b) the high temperature phase obtained by heating for 72 h; (c) ammonolysis of metallorganic precursor.

may provide insight into the oxidation states of individual atoms in these compounds. An attempt was made to synthesize other members of the series with Cu, Zn, Cd, and Pb in place of nickel. The AWO_4 (A = Cu, Zn, Cd, and Pb) precursors were prepared and heated in ammonia at different temperatures; when heated below 600 °C they yielded high surface area W_2N and metal (A) particles.

Bem *et al.* have reported the synthesis of Ni_3Mo_3N from ammonolysis of $NiMoO_4$.[5] Our recent investigation confirmed

Table 4 X-Ray powder diffraction data for the NiW_3N phase [unit cell parameters $a = 5.799(1)$ Å, $b = 5.827(1)$ Å and $c = 8.245(2)$ Å]

h	k	l	d_{calc}/Å	d_{obs}/Å	I/I_o
0	0	2	4.122	4.093	35
1	1	2	2.910	2.907	39
1	2	0	2.603	2.569	5
2	1	0	2.595		
1	0	3	2.483	2.504	9
1	2	1	2.482	2.475	13
2	1	1	2.476		
0	2	2	2.379	2.371	100
2	0	2	2.371		
2	2	0	2.055	2.055	88
0	0	4	2.061		
3	0	1	1.882	1.873	5
1	1	4	1.842	1.838	13
1	3	1	1.797	1.784	12
3	1	1	1.790		
1	3	2	1.681	1.678	15
3	1	2	1.676		
2	2	4	1.455	1.454	37
4	0	0	1.449	1.447	5
1	3	4	1.373	1.370	6
3	1	4	1.370		
3	3	2	1.300	1.300	5
1	4	3	1.256	1.261	7
2	4	2	1.241	1.240	29
4	2	2	1.238		

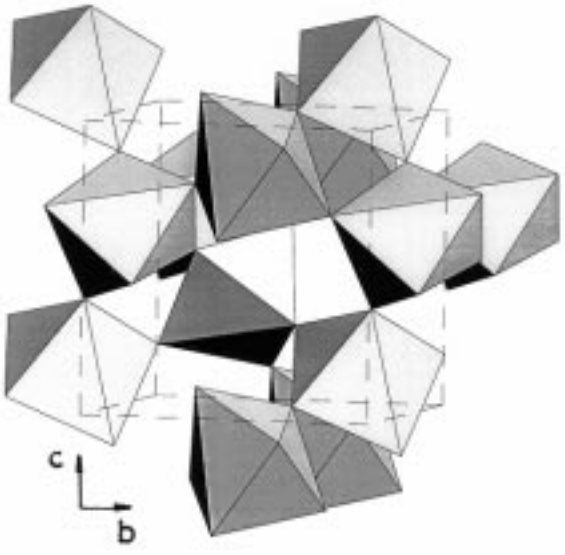

Fig. 8 The structure of Ni_2W_3N showing corner-shared $[NW_6]$ polyhedra. The nickel atoms are not shown.

that the composition suggested in the work of Bem *et al.* was not accurate, and the composition turned out be a mixture of Ni_2Mo_3N [β-Mn structure, $a = 6.6521(5)$ Å] and Ni impurity.[23] While Ni_2W_3N decomposed at higher temperatures to phase (II), Ni_2Mo_3N was not converted into any new phases. The phase diagrams and structures of these ternary intermetallic nitrides thus continue to pose several interesting questions, particularly regarding their stability and local electronic structures. It is, therefore, likely that an adequate rationalization of the observed interesting structures will be provided only by detailed band structure calculations.

Magnetic susceptibility of Ni_2W_3N shows paramagnetic behaviour. Since the sample contained small amounts of Ni impurity, further investigations using pure Ni_2W_3N are essential to establish the magnetic properties of the sample. It is interesting to note that Fe_3Mo_3N showed paramagnetic behaviour and orders antiferromagnetically with a Néel temperature $T_N = 120$ K.[24] Resistivity measurements of Ni_2W_3N and the

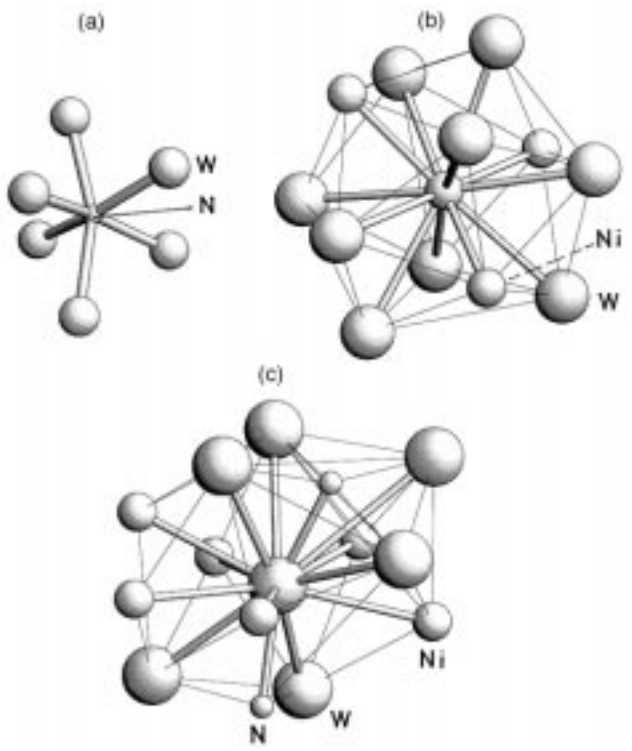

Fig. 9 The coordination of neighboring atoms about each of three different atoms in Ni_2W_3N. (a) The $[NW_6]$ distorted octahedra; (b) $Ni[Ni_3W_9]$ pseudo-icosahedra; (c) $W[N_2Ni_6W_6]$ pseudo-tetradecahedra.

new phase were recorded using pressed pellets; both the samples showed metallic behavior.

Conclusions

We have synthesized and characterized a new intermetallic nitride, Ni_2W_3N. This nitride crystallizes in a filled β-Mn structure and is isostructural with Al_2Mo_3C. Ni_2W_3N decomposed to give a new phase related to the distorted anti-perovskite structure on prolonged heating in ammonia. This work confirms that although carbides and nitrides have been considered together in the literature on the basis of similarities in structure and properties, there are some interesting exceptions amongst these two classes of compounds. Low temperature methods are particularly attractive for producing intermetallic phases because they provide an opportunity to examine some previously inaccessible low temperature areas of phase diagrams.

References

1 L. E. Toth, in *Transition metal carbides and nitrides*, Academic Press, New York, 1971, vol. 7.
2 Z. Altounian, X. Chen, L.X. Liao, D. H. Ryan and J.O. Ström-Olsen, *J. Appl. Phys.*, 1993, **73**, 6017.
3 F. J. DiSalvo, *Science*, 1990, **247**, 649.
4 S. H. Elder, F. J. DiSalvo, L. Topor and A. Navrotsky, *Chem. Mater.*, 1993, **5**, 1545.
5 D. S. Bem, C. P. Gibson and H.-C. zur Loye, *Chem. Mater.*, 1993, **5**, 397.
6 P. S. Herle, N. Y. Vasanthacharya, M. S. Hegde and J. Gopalakrishnan, *J. Alloys Compd.*, 1995, **217**, 22.
7 K. S. Weil and P. N. Kumta, *Acta Crystallogr., Sect. C*, 1997, **53**, 1745.
8 E. Matijevic, M. Kerker, H. Beyer and F. Theubert, *Inorg. Chem.*, 1963, **2**, 581.
9 K. S. Weil and P. N. Kumta, *J. Solid State Chem.*, 1997, **128**, 185.
10 M. S. Hegde, S. Ramesh and G. S. Ramesh, *Proc. Ind. Acad. Sci. (Chem. Sci.)*, 1992, **104**, 34.
11 W. Losocha and K. Lewinski, *J. Appl. Crystallogr.*, 1994, **27**, 437.
12 H. M. Rietveld, *J. Appl. Crystallogr.*, 1969, **2**, 65.
13 M. L. Fiedler and H. Stadelmaier, *Z. Metallkd.*, 1975, **66**, 402.
14 H. H. Stadelmaier, in *Developments in the Structural Chemistry of Alloy Phases*, ed. B. C. Giessen, Plenum Press, New York, 1969, p. 141.
15 P. Villars and L. D. Calvert, *Pearson Handbook of Crystallographic Data for Intermetallic Phases*, ASM International, USA, 2nd edn., 1991, 1991, vol. 1–4.
16 J. L. C. Daams, P. Villars and J. H. N. van Vucht, *Atlas of Crystal Structure Types for Intermetallic Phases*, ASM International, USA, 1991, vol. 4.
17 J. D. Houmes. D. S. Bem and H.-C. zur Loye, *Mater. Res. Soc. Symp. Proc.*, 1994, **327**, 153.
18 W. Jeitschko, H. Nowotny and F. Benesovsky, *Mh. Chem. Bd.*, 1963, **94**, 247.
19 M. Y. Chern, F. J. DiSalvo, J. B. Parise and J. A. Goldstone, *J. Solid State Chem.*, 1992, **96**, 426.
20 J. S. Kasper and B. W. Roberts, *Phys. Rev.*, 1956, **101**, 537.
21 W. B. Pearson, in *Developments in the Structural Chemistry of Alloy Phases*, ed. B. C. Giessen, Plenum Press, New York, USA, 1969, p. 1.
22 P. Subramanya Herle, M. S. Hegde, K. Sooryanarayana, T. N. Guru Row and G. N. Subbanna, unpublished work.
23 A. F. Wells, *Structural Inorganic Chemistry*, Oxford University Press, New York, 5th edn., 1984, 5th p. 584.
24 R. N. Panda and N. S. Gajbhiye, *J. Alloys Compd.*, 1997, **256**, 102.

Paper 8/00298C; *Received* 12*th January*, 1998